*J. Fluid Mech.* (1966), *vol.* 24, *part* 2, *pp.* 255–274
*Printed in Great Britain*



# The effects of pressure gradients on turbulent flow near a smooth wall

By GEORGE L. MELLOR
Department of Aerospace and Mechanical Sciences, Princeton University

(Received 29 June 1964 and in revised form 31 March 1965)

A dimensional argument is presented leading to a functional form for the effective viscosity which embraces the hypothesis of a previous paper (Mellor & Gibson 1966; hereafter referred to as paper A) in the defect portion of a turbulent boundary layer. The new argument also suggests a way of determining the effective viscosity in the viscous sublayer when the flow is subjected to mainstream pressure gradients.

It will be shown that the large wall-velocity profiles and the defect-velocity profiles automatically overlap, even in the absence of a logarithmic portion. It will be shown further that equilibrium flows are uniquely determined by $\beta$ and **R**.

## 1. Introduction

In the preceding paper (Mellor & Gibson 1966) it was shown that the adoption of the Boussinesq definition of an effective viscosity, $\nu_e$, whereby

$$\tau/\rho = \nu_e(\partial u/\partial y), \tag{1}$$

together with some assumptions concerning $\nu_e$, led to a rather complete store of information concerning equilibrium turbulent boundary layers which is in good agreement with experiment.

Paper A was largely concerned with the defect portion of equilibrium boundary layers. As long as the parameter $\beta \equiv (\delta^* dp/dx)/\tau_0$ is small, the defect profiles are logarithmic for small enough $y$ and may be matched with the logarithmic portion of the law of wall. In this way, the defect profile may be related to the true wall condition $u(y = 0) = 0$, and, at the same time, the skin-friction coefficient may be determined. However, when $\beta$ is large, one finds that (for some Reynolds number) there is no portion of the defect profile which overlaps the logarithmic portion of the law of the wall. Conversely, under the same conditions, it is fair to presume that the logarithmic portion of the law of the wall actually ceases to exist. In §§ 7 and 8 of paper A we circumvented this difficulty in a way which rather lacks conviction, and it is our present intention to repair this deficiency.

Although the present paper and paper A will be interrelated, some of the results presented herein will be more general in that they attempt to assess the effect of pressure gradients on the velocity distribution near a smooth wall without restriction to equilibrium boundary layers ($\beta(x) = \text{const.}$).

At the outset the basic effective-viscosity hypothesis of paper A is reviewed in

the light of a similarity argument, and the hypothesis is extended to include the viscous sublayer immediately adjacent to the wall. The similarity argument is also applied to other hypotheses that have appeared in the literature.

## 2. Notation

The notation includes symbols defined in Mellor & Gibson (1965). Additional symbols are:

$\phi = \nu_e/\nu$, ratio of effective viscosity to molecular viscosity;
$\zeta = (\kappa^2 y^2/\nu)\,|\partial u/\partial y|$;
$u_{p\nu} = [(\nu/\rho)\,(dp/dx)]^{\frac{1}{3}}$, pressure-viscosity velocity;
$y^+ = yu_\tau/\nu$;
$u^+ = u/u_\tau$;
$y^* = yu_{p\nu}/\nu$;
$u^* = u/u_{p\nu}$;
$\alpha = \nu(dp/dx)/\rho u_\tau^3 = (u_{p\nu}/u_\tau)^3$, wall-layer parameter.

## 3. A dimensional argument for the behaviour of $\nu_e$

We shall first present a skeleton exposition of the argument and then provide further discussion. At the outset we note that arguments of this type have been applied by Millikan (1938) to deduce the logarithmic behaviour of the velocity profile near a wall (and by Kolmogoroff in his treatment of homogeneous turbulence). A necessary assumption of the present discussion will be that $\nu_e$ depends on only three physical quantities in the wall layer.

The similarity argument may be considered in two steps:

(i) Assume that in the wall layer, $\nu_e = \nu_e(y, u', \nu)$, where, here, $u' \equiv \partial u/\partial y$. In the defect layer, assume $\nu_e = \nu_e(y, u', U\delta^*)$. The important feature of this assumption is that $\nu_e$ is independent of the molecular viscosity in the defect layer but depends on $U\delta^*$ as well as $y$ and $u'$. It is implicit that, here, $\nu_e$ depends only on velocities relative to the main stream since

$$U\delta^* = \int_0^\infty (U-u)\,dy$$

and $u' = -\partial(U-u)/\partial y$. Non-dimensionally we have

$$\frac{\nu_e}{\nu} = \phi\left(\frac{y^2u'}{\nu}\right) \quad \text{in the wall layer,} \tag{2a}$$

and

$$\frac{\nu_e}{U\delta^*} = \Phi\left(\frac{y^2u'}{U\delta^*}\right) \quad \text{in the defect layer.} \tag{2c}$$

$\phi$ is presumed to be universally applicable near a smooth wall. $\Phi$ is presumed to be universally applicable in the outer part of the turbulent boundary layer, but does depend on the fact of it being a boundary layer. For example, some other function, $\Phi'$, might apply to fully-developed pipe flow.

(ii) We now hypothesize the existence of an overlap layer where $\phi$ and $\Phi$ are both valid. Then we have $\nu_e = \nu\phi = U\delta^*\Phi$, and it follows that

$$\nu_e = \kappa^2 y^2 u', \tag{2b}$$

for the overlap layer. At this point $\kappa^2$ is an arbitrary constant.

The above argument is far from being a derivation based on first principles, but it does systematize our thinking and clarify certain concepts. Prandtl's 'mixing length hypothesis' (equation (2*b*)) is now viewed as the overlap *portion* of the function $\phi$, which we know must also approach the value 1 as its argument approaches 0. It is also the overlap *portion* of the function $\Phi$, which, according to Clauser's hypothesis (or analytical approximation), in the case of equilibrium boundary layers becomes equal to $K$ (see paper A) for some large value of its argument.

One further comment is in order. In equation (2*c*), $\Phi$ could also be considered a function of $\beta$. But the Clauser hypothesis, which received strong support in paper A, stated that, nevertheless, $\Phi = K$ for all values of $\beta = \text{const.}$ However, for non-equilibrium boundary layers where $\beta = \beta(x) \neq \text{const.}$, we have no further basis for this simplification; in other words, $\Phi$ could conceivably depend on $\beta(x)$. In any event we would nevertheless obtain equation (2*b*) in the overlap layer. This seems to be verified experimentally for non-equilibrium cases (at least when $\tau \simeq \tau_0$ near the wall), and is apparently a consequence of the small effect exerted by the inertial terms in the momentum equation near the wall.

### *Alternatives to equation* (2)

The derivation of equation (2) is not unique. It depends on the initial choice of physical quantities which one deems to be pertinent near a wall and away from the wall. Rather than attempt to justify this choice with lengthy physical arguments, we shall here simply fall back on the observation that equations (2*b*, *c*) led to accurate predictions of defect-velocity profiles for a large range of equilibrium boundary layers.† But, let us, at least, examine other possibilities.

I. In (i) assume that in the wall layer $\nu_e = \nu_e(y, u_\tau, \nu)$, and in the defect layer $\nu_e = \nu_e(y, u_\tau, U\delta^*)$. We then obtain

$$\nu_e/\nu = \phi(yu_\tau/\nu) \quad \text{in the wall layer,}$$

$$\nu_e/U\delta^* = \Phi(yu_\tau/U\delta^*) \quad \text{in the defect layer,}$$

and

$$\nu_e/\nu = \kappa y u_\tau/\nu \quad \text{in the overlap layer.}$$

This last result corresponds to one of Clauser's assumptions mentioned in paper A. There we found that it is acceptable only if $\tau \simeq \tau_0$ in the overlap layer, in which case it is equivalent to equation (2*b*).

II. In (i) assume that in the wall layer $\nu_e = \nu_e(y, u, \nu)$, and in the defect layer $\nu_e = \nu_e(y, u, U\delta^*)$. We then obtain

$$\nu_e/\nu = \phi(yu/\nu) \quad \text{in the wall layer,}$$

$$\nu_e/U\delta^* = \Phi(yu/U\delta^*) \quad \text{in the defect layer,}$$

and

$$\nu_e \propto uy \quad \text{in the overlap layer.}$$

When $\tau \simeq \tau_0$ this does not predict a logarithmic behaviour in the overlap region and is unacceptable.

† Equation (2) also works very well in predicting pipe flows, where, however, $\Phi = K$ is not equal to 0·016 in the outer layer. Other values of $K$ are appropriate to free turbulent flows, etc.

III. In (i) assume that in the wall layer $\nu_e = \nu_e(u', u'', \nu)$, and in the defect layer $\nu_e = \nu_e(u', u'', U\delta^*)$. We then obtain

$$\nu_e/\nu = \phi(u'^3/u''^2\nu), \quad \text{in the wall layer,}$$
$$\nu_e/U\delta^* = \Phi(u'^3/u''^2 U\delta^*) \quad \text{in the defect layer,}$$
and
$$\nu_e = \kappa^2 u'^3/u''^2 \quad \text{in the overlap layer.}$$

This latter result is von Karman's similarity hypothesis. It succeeds in predicting a logarithmic portion in the overlap layer when $\tau \simeq \tau_0$. When $\tau_0 = 0$ and $\tau \simeq (dp/dx)y$, we obtain $u \sim y^{\frac{1}{2}}$, but the constant of proportionality differs by a factor of 2 over that obtained with equation (2c). Stratford's data for this case does appear to represent an experimental judgement in opposition to the von Karman result. Furthermore, very near the wall, $\nu u'' = (1/\rho)(dp/dx)$. $\phi$ and therefore $u$ would depend strongly on the pressure gradient even when it is weak (the argument of $\phi$ would become infinite for zero pressure gradient). Based on experimental observation this is an unacceptable result.

Other hypotheses that attempt to characterize the effective viscosity in the sublayer generally fall into one or combinations of the above categories (e.g. Deissler 1959; van Driest 1956), and are applicable only when $\tau \simeq \tau_0$; with the help of the relation $\tau = \tau_0$, all of these hypotheses may be transformed to the simplest form $\nu_e/\nu = \phi(yu\tau/\nu)$.

## 4. The complete effective viscosity function

After the above diversion we resume the analysis related to equation (2). We set

$$\zeta = \frac{\kappa^2 y^2}{\nu}\left|\frac{\partial u}{\partial y}\right|, \tag{3a}$$

$$Z = \frac{\kappa^2 y^2}{U\delta^*}\left|\frac{\partial u}{\partial y}\right|, \tag{3b}$$

(We here require that $\nu_e$ and therefore $\zeta$ be positive. In the present paper $\partial u/\partial y$ is always positive, and we shall sometimes drop the symbol $|\ |$.)

We can accordingly summarize the information so far available as follows:

$$\left.\begin{aligned} &\phi \sim 1 \quad \text{as} \quad \zeta \to 0, \\ &\phi = \zeta \quad \text{in the overlap layer,} \end{aligned}\right\} \tag{4a}$$

$$\Phi = \begin{cases} Z(\eta) & (\eta \leqslant e), \\ K & (\eta \geqslant e), \end{cases} \tag{4b}$$

where $e$ is the smaller root where $Z(e) = K$. Equation (4b) is a well-defined function and was the basis of paper A.

It remains therefore to determine a specific function $\phi(\zeta)$, which satisfies the known conditions given in equation (4a). Once this is determined the complete effective viscosity function may be described in terms of either $\phi$ or $\Phi$ since

$$\phi(\zeta)/\mathbf{R} = \Phi(Z), \quad \zeta = \mathbf{R}Z, \tag{5a,b}$$

everywhere and $\mathbf{R} \equiv U\delta^*/\nu$.

It is apparent that $\phi(\zeta)$ might be evaluated from the experimental 'law of the wall' for the case where $\tau \simeq \tau_0$ in the wall layer. If we let $u^+ = u/u_\tau$ and $y^+ = yu_\tau/\nu$ equations (1) and (3*a*) may be written in the form

$$\phi(\zeta)\,\partial u^+/\partial y^+ = 1, \quad \zeta = \kappa^2 y^{+2}\,\partial u^+/\partial y^+. \tag{6a, b}$$

Apparently there is a limited amount of boundary-layer data which is clearly valid in a region including the viscous sublayer. We have therefore appealed to Laufer's (1954) pipe data, which is attractive since it exhibits the correct asymptotic behaviour $u^+ \sim y^+$ as $y^+ \to 0$. For this reason and for the reason that the viscous sublayer is thickest for small Reynolds number we have favoured the data points for $Ua/\nu = 50{,}000$ rather than for 500,000 as shown in figure 1.

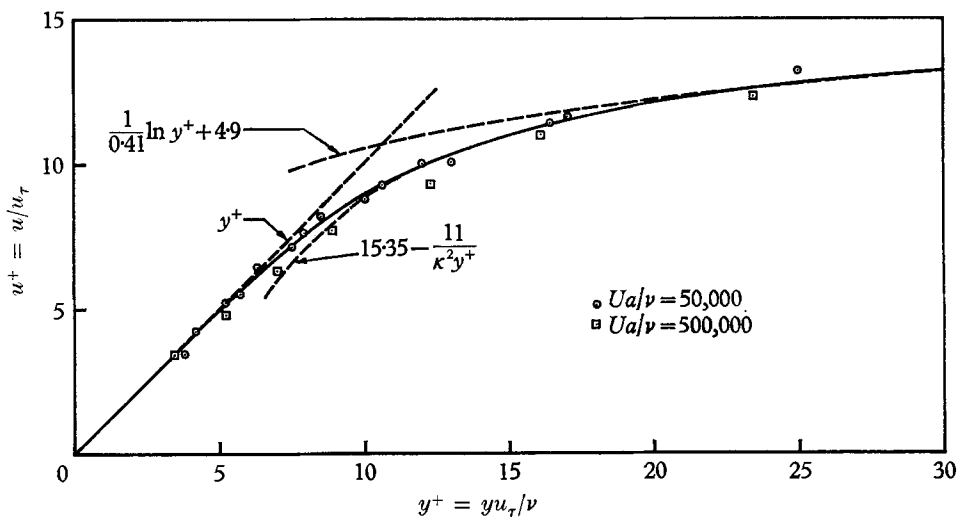


FIGURE 1. Comparison of calculated profile (solid line) and data in the wall layer. Data are from Laufer (1954).

There are two ways of determining the slopes, $\partial u^+/\partial y^+$, and then $\phi(\zeta)$: by graphical differentiation or by differentiating an analytical function which passes through the data points. As long as $y^+ > 27$ the logarithmic law of the wall passes through the data and immediately we have $\phi = \zeta$ for $\zeta > 11$; for very small $y^+$ we have $u^+ = y^+$ and $\phi = 1$.† In the intermediate range we differentiated the experimental data of figure 1 graphically and found that $\phi(\zeta)$ increased very abruptly at about $\zeta = 11$; the detailed nature of the curve was very sensitive to slight changes in the graphical measurements. In fact, if we let

$$\zeta = \kappa^2 y^{+2}\,du^+/dy^+ = 11$$

we obtain $u^+ = C - (11/\kappa^2)/y^+$. By setting $C = 15{\cdot}35$ the curves fit the data in the range $12 \leqslant y^+ \leqslant 27$ and fair with the logarithmic curve at $y^+ = 27$.

† Moreover, it is known that $u^+ = y^+ + a_4 y^{+4} + \ldots$ as $y^+ \to 0$ (Townsend 1956, Chapter 9). The truncated 2-term expression applies only in the range $0 \leqslant y^+ \leqslant 6$ (with $a_4 = 1{\cdot}2$), however.

$\phi(\zeta)$, plotted in figure 2, is the net result of these considerations and the solid curve drawn in figure 1 is actually obtained by re-integrating this result (see §6).

We note that recently van Driest & Blumer (1963) have proposed the parameter $(y^2/\nu)\,(\partial u/\partial y)$ as the basis for a criterion for transition of laminar boundary layers;

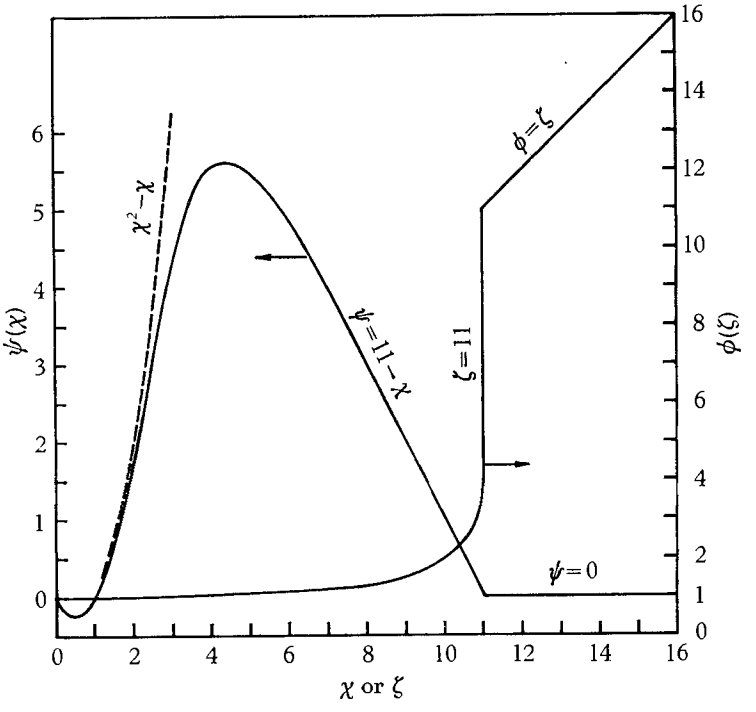


FIGURE 2. The effective viscosity function $\phi(\zeta)$, and the function $\Psi(\chi)$.

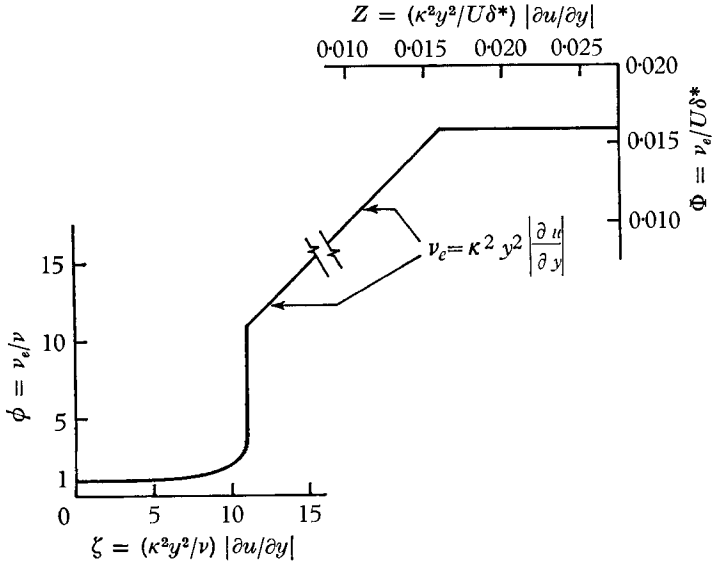


FIGURE 3. The composite effective viscosity function. Prandtl's relation is viewed as a consequence of the overlap of $\phi(\zeta)$ and $\Phi(Z)$.

the effective value of the parameter decreases with free-stream turbulence. It is possible that the value $(y^2/\nu)(\partial u/\partial y) = 11/\kappa^2$ represents a value below which all disturbances are damped.

In figure 3 we have plotted $\phi(\zeta)$ and on the same plot superimposed the function $\Phi(Z)$ for equilibrium boundary layers. Either of the complete functions, $\phi(\zeta)$ or $\Phi(Z)$, valid everywhere, could be determined according to equations $(5a, b)$ after stipulating $\mathbf{R}$.

A lower limit of $\mathbf{R}$ for the validity of our entire analysis is implied by figure 3. No overlap exists when $11\nu > KU\delta^*$ or, with $K = 0{\cdot}016$, when $\mathbf{R} < 700$. The value $\mathbf{R} = 700$ is generally lower than the Reynolds number of transition.

## 5. The complete solution

By stipulating $\beta$ and the additional parameter $\mathbf{R}$ it would be possible to repeat the entire calculations of paper A using a complete $\Phi(Z)$ as derived from figure 3. Since $f'(\eta) = (U-u)/u_\tau$ would, in all cases, now be regular at $\eta = 0$ a direct result of such a calculation would be the skin-friction coefficient, $(2/c_f)^{\frac{1}{2}} = U/u_\tau = f'(0)$ corresponding to the wall condition $u(0) = 0$. Calculations for a range of $\beta$ and $\mathbf{R}$ could be made to provide a complete store of information.

However, there are conceptual and analytical advantages in dividing the profile into a defect form (dependent on $\beta$), and a wall form (which will involve a new pressure gradient parameter). To achieve this division it is necessary to make the analytical approximation of neglecting inertial terms in the wall layer. Otherwise the result would again be of both $\beta$ and $\mathbf{R}$. A detailed examination of the range of validity of this approximation will be made at the end of § 6.

## 6. The wall profiles

It is first possible to derive a convenient, general integral equation involving the total stress. From equations (1), $(2a)$ and $(3a)$ we can write

$$\nu\phi(\zeta)\,\partial u/\partial y = \tau/\rho,$$

or
$$\zeta\phi(\zeta) = \chi^2, \tag{7}$$

where we define
$$\chi = (\tau/\rho)^{\frac{1}{2}}\kappa y/\nu. \tag{8}$$

(Adhering to the strict definition of $\zeta$ in $(3a)$ equation (7) should be written more generally as $\zeta\phi(\zeta) = \chi^2\,\mathrm{sgn}\,(\tau)$ where $\chi = |\tau/\rho|^{\frac{1}{2}}\kappa y/\nu$. In the present paper we require that $\tau$ be positive.) Now equation (7) may be inverted so that $\zeta$ is expressed as some function of $\chi$. For a reason that will shortly be apparent we choose to write this inverted equation in the form

$$\zeta = \psi(\chi) + \chi. \tag{9}$$

The function $\psi(\chi)$ can be determined from $\phi(\zeta)$ and equations (7) and (9) and is plotted in figure 2. Recalling the definition of $\zeta$ we can write

$$\frac{\kappa^2 y^2}{\nu}\frac{\partial u}{\partial y} = \psi(\chi) + \left(\frac{\tau}{\rho}\right)^{\frac{1}{2}}\frac{\kappa y}{\nu},$$

which has the solution

$$u = \lim_{\epsilon\to 0}\left[\int_\epsilon \frac{\nu\psi(\chi)}{\kappa^2 y^2}\,dy - \frac{u_\tau}{\kappa}\ln\frac{\epsilon u_\tau}{\nu}\right] + \lim_{\epsilon\to 0}\left[\int_\epsilon \frac{(\tau/\rho)^{\frac{1}{2}}}{\kappa y}\,dy + \frac{u_\tau}{\kappa}\ln\frac{\epsilon u_\tau}{\nu}\right]. \tag{10}$$

We have arranged equation (10) in the above form since, when $\tau \simeq \tau_0$, the second term on the right yields the familiar $(1/\kappa)\ln yu_\tau/\nu$; the first term represents departure from the logarithmic behaviour in the sublayer and if the integration is carried to a value of $y$ outside the viscous sublayer where $\psi(\chi) = 0$ the first term should yield the constant value 4·9. It should be clear that, although these remarks apply when $\tau \simeq \tau_0$, equation (10) is applicable even when this restriction is not imposed, in which case the second term may not be logarithmic and the first term will be constant outside the viscous sublayer but will not, in general, be equal to 4·9.

In a region which includes the viscous sublayer and at least a part of the overlap layer we now make the approximation that

$$\tau/\rho = u_\tau^2 + Py, \tag{11}$$

where $u_\tau^2 = \tau_0/\rho$ and we have temporarily set $P = (1/\rho)(dp/dx)$. Equation (11) assumes that the inertial terms in the equations of motion can be neglected. Very near the wall the approximation is obviously valid; later, we shall determine the outer limit of $y$ within which the approximation is valid and the nature of the join between the resulting solutions and the defect solutions of paper A.

Together with equation (11) the second term on the right in equation (10) can be integrated and the result is

$$u = \lim_{\epsilon\to 0}\left[\int_\epsilon \frac{\nu\psi(\chi)}{\kappa^2 y^2}dy - \frac{u_\tau}{\kappa}\ln\frac{\epsilon u_\tau}{\nu}\right] + \frac{2}{\kappa}[(u_\tau^2+Py)^{\frac{1}{2}} - u_\tau] + \frac{u_\tau}{\kappa}\ln\left[4\frac{u_\tau^3}{\nu P}\frac{(u_\tau^2+Py)^{\frac{1}{2}} - u_\tau}{(u_\tau^2+Py)^{\frac{1}{2}} + u_\tau}\right]. \tag{12}$$

Equation (12) may be written in two different forms depending on whether the parameter $\alpha \equiv \nu P/u_\tau^3$ is large or small.

For small $\alpha$ we have

$$u^+ = u_v^+ + \frac{2}{\kappa}[(1+\alpha y^+)^{\frac{1}{2}} - 1] + \frac{1}{\kappa}\ln\left[\frac{4}{\alpha}\frac{(1+\alpha y^+)^{\frac{1}{2}} - 1}{(1+\alpha y^+)^{\frac{1}{2}} + 1}\right], \tag{13a}$$

where $y^+ = yu_\tau/\nu$, $u^+ = u/u_\tau$ and

$$u_v^+ \equiv \lim_{\epsilon\to 0}\left[\int_\epsilon \frac{\psi(\chi)}{\kappa^2 y^2}dy^+ - \frac{\ln\epsilon}{\kappa}\right]. \tag{13b}$$

We also find that $\chi = \kappa(1+\alpha y^+)^{\frac{1}{2}}y^+$. Outside the viscous sublayer $u_v^+ = B^+(\alpha)$, a constant.

For large $\alpha$ we have

$$u^* = u_v^* + \frac{2}{\kappa}[(\alpha^{-\frac{2}{3}} + y^*)^{\frac{1}{2}} - \alpha^{-\frac{1}{3}}] + \frac{1}{\kappa\alpha^{\frac{1}{3}}}\ln\left[\frac{4}{\alpha}\frac{(\alpha^{-\frac{2}{3}}+y^*)^{\frac{1}{2}} - \alpha^{-\frac{1}{3}}}{(\alpha^{-\frac{2}{3}}+y^*)^{\frac{1}{2}} + \alpha^{-\frac{1}{3}}}\right], \tag{14a}$$

where, if $u_{p\nu} = (\nu P)^{\frac{1}{3}}$, $y^* = yu_{p\nu}/\nu$ and $u^* = u/u_{p\nu}$ and

$$u_v^* = \lim_{\epsilon\to 0}\left[\int_\epsilon \frac{\psi(\chi)}{\kappa^2 y^{*2}}dy^* - \frac{1}{\kappa\alpha^{\frac{1}{3}}}\ln\frac{\epsilon}{\alpha^{\frac{1}{3}}}\right]. \tag{14b}$$

Also $\chi = \kappa(\alpha^{-\frac{2}{3}} + y^*)^{\frac{1}{2}}y^*$. Outside the viscous sublayer, $u_v^* = B^*(\alpha) = B^+/\alpha^{\frac{1}{3}}$, a constant.

Equation (13) has a simple limit at $\alpha = 0$ and approaches $(1/\kappa)\ln y^+ + B^+$ when $y^+ \ll \alpha^{-1}$. Equation (14) has a simple limit at $1/\alpha = 0$ and approaches $(2/\kappa)y^{*\frac{1}{2}} + (1/\kappa\alpha^{\frac{1}{3}})[\ln(4/\alpha) - 2] + B^*$, when $y^* \gg \alpha^{-\frac{2}{3}}$.

The functions $u_v^+(y^+)$ and $u_v^*(y^*)$ were determined numerically for a range of $\alpha$. $B^+$ or $B^*$ is plotted in figure 4 and listed in table 1. The detailed behaviour of $B^*$

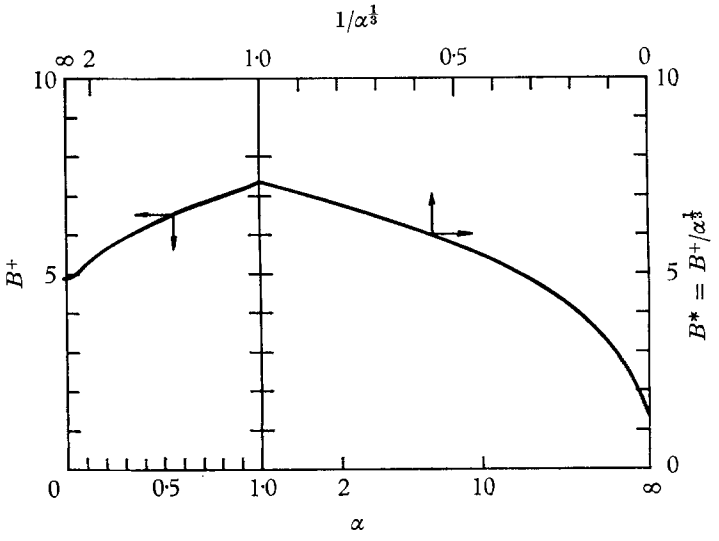


FIGURE 4. The numerically determined $B^+$ or $B^*$.

| $\alpha$ | $B^+$ | $1/\alpha$ | $B^*$ |
|---|---|---|---|
| −0·01 | 4·92 | 0 | 1·33 |
| 0 | 4·90 | 0·1 | 5·63 |
| 0·02 | 4·94 | 0·5 | 6·74 |
| 0·05 | 5·06 | 1·0 | 7·34 |
| 0·10 | 5·26 | 2·0 | 8·12 |
| 0·20 | 5·63 | 3·0 | 8·70 |
| | | 4·0 | 9·18 |
| | | 5·0 | 9·62 |

Note: equation (32) is an analytical expression for $B^*(\alpha)$ valid in the range $0 \leqslant 1/\alpha \leqslant 0{\cdot}01$.

TABLE 1. Values of $B^+$ or $B^* = B^+/\alpha^{\frac{1}{3}}$

for large $\alpha$ is examined in appendix A. The complete solutions are plotted in figure 5 (*a*) for small $\alpha$ and in figure 5 (*b*) for large $\alpha$.

Ferrari (1956) and Townsend (1961) have already derived equations similar in form to equation (13) applicable only outside the viscous sublayer. However, $B^+$ has been assigned the constant value appropriate to $\alpha = 0$ so that their results are in error for large $\alpha$.

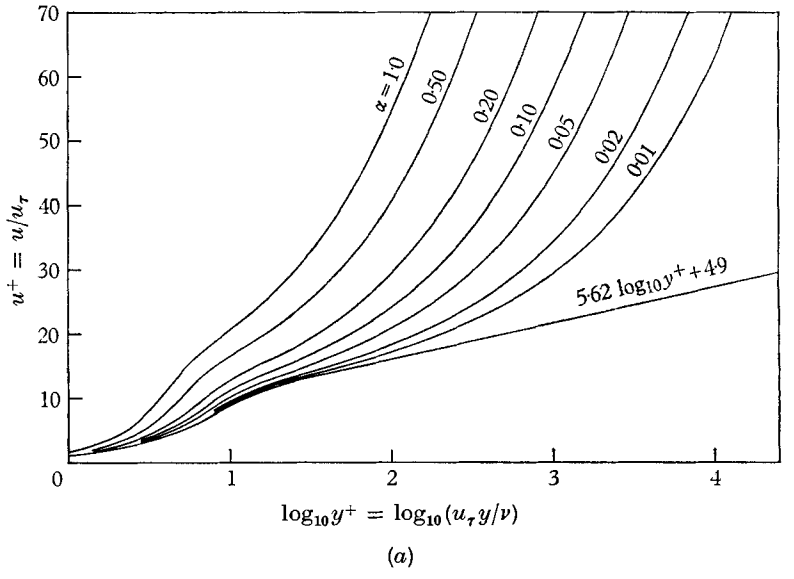


(a)

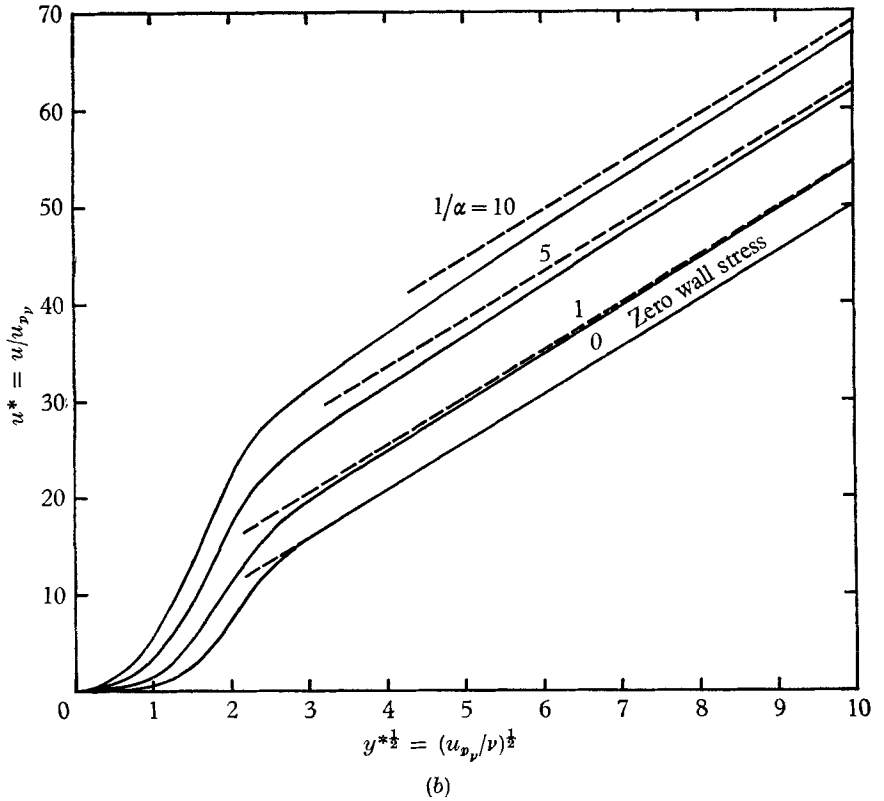


(b)

FIGURE 5. (a) $u^+$ *vs* $y^+$ for small $\alpha$. The conventional 'law of the wall' is only valid for very small $\alpha$. Since $\beta = \alpha\gamma\mathbf{R}$, small $\alpha$'s can nevertheless correspond to fairly large $\beta$'s. (b) $u^*$ *vs* $y^*$ for large $\alpha$. The broken lines are $u^* = \text{const.} + (2/\kappa)y^{*\frac{1}{2}}$.

*Relationship between the wall profiles and the defect profiles*

The defect profiles of paper A are calculated on the basis of an effective viscosity which vanishes at the origin and, of course, this is unrealistic in the viscous sublayer. On the other hand, the wall profiles should be correct in the viscous sublayer but are incorrect in the outer layer on two counts: the effective viscosity increases indefinitely and the effective stress variation does not include inertial effects.

In the overlap region the effective viscosity distributions of both analyses are identical ($\nu_e = \kappa^2 y^2 |\partial u/\partial y|$). If there is a region within the overlap layer where the shear stress distribution calculated in paper A is, at least, approximated by equation (11) then we can conclude that, in this region, the velocity profiles of both analyses will overlap. We will see that this later condition is not analytically obvious so that it is desirable to devote the remainder of this section to a demonstration of the fact that $\tau$ of paper A is, in a very real sense, approximated by equation (11) within the overlap layer for all values of $\beta$.

For convenience let us denote the $\tau$ distribution of paper A as $\tau_A$ and the $\tau$ distribution of the present paper as $\tau_B$. Equation (11) can then be written

$$\frac{\tau_B}{\tau_0} = 1 + \frac{\beta}{\gamma}\eta \quad \text{or} \quad \frac{\partial(\tau_B/\tau_0)}{\partial\eta} = \frac{\beta}{\gamma}, \tag{11'}$$

for direct comparison with $\tau_A/\tau_0$.

A modified momentum equation may be adopted to present $\tau_A$ in the form

$$\frac{\partial\tau_A}{\partial y} = u\frac{\partial u}{\partial x} - U\frac{dU}{dx}. \tag{15}$$

It can be shown that equation (15) is correct as $y \to 0$. As in paper A we now set $u = U(1-\gamma f')$ and also $\partial u/\partial x = U'(1-\gamma f')$. It is permissible to neglect $\gamma' = d\gamma/dx$; inclusion of this term would complicate the algebra but would not alter our conclusions. Insertion of the above results in equation (15) yields† $\partial\tau_A/\partial y = UU'(1-\gamma f')^3 - UU'$, which can be written

$$\frac{\partial(\tau_A/\tau_0)}{\partial\eta} = \frac{\beta}{\gamma}[1-(1-\gamma f')^2],$$

or

$$\frac{\partial(\tau_A/\tau_0)}{\partial\eta} = \beta(2f' - \gamma f'^2). \tag{16}$$

For small $\eta$, $f' = A - (1/\kappa)\ln\eta$ and it is difficult to see how equations (11') and (16) compare.

Now let us determine the point, $y_0$, at which equations (11') and (16) agree. This clearly occurs when

$$1/\gamma = f'(\eta_0) = A - \kappa^{-1}\ln\eta_0. \tag{17}$$

In § 7 we shall show that the skin-friction equation may be written

$$\frac{1}{\gamma} = \frac{1}{\kappa}\ln\frac{U\delta^*}{\nu} + A + B^+. \tag{18}$$

† Or $\partial\tau_A/\partial y = (dp/dx)(1-u^2/U^2)$, which shows clearly how the local inertial terms modify equation (11). To be exact in the limit as $y \to 0$ the effect of $\gamma'$ should be included.

Combining equations (17) and (18) yields $\ln(y_0 u_\tau/\nu) = -\kappa B^+$, or

$$y_0^+ = \exp(-\kappa B^+). \tag{19}$$

Thus we see that $\partial\tau_A/\partial y = \partial\tau_B/\partial y$ deep in the viscous sublayer even though the behaviour of these quantities are analytically dissimilar as $y \to 0$.

It is now possible to understand the relative behaviour of $\tau_A$ and $\tau_B$. Even though $\partial\tau_A/\partial y$ is infinite at $y = 0$,† nevertheless, $\partial\tau_A/\partial y = \partial\tau_B/\partial y$ in the viscous sublayer; at this point $\tau_A$ is only slightly larger than $\tau_B$. $\partial\tau_A/\partial y$ then slowly decreases so that $\tau_A = \tau_B$ again at some value of $y$. This value of $y$ could be designated as the matching *point* where also $\partial u_A/\partial y = \partial u_B/\partial y$.

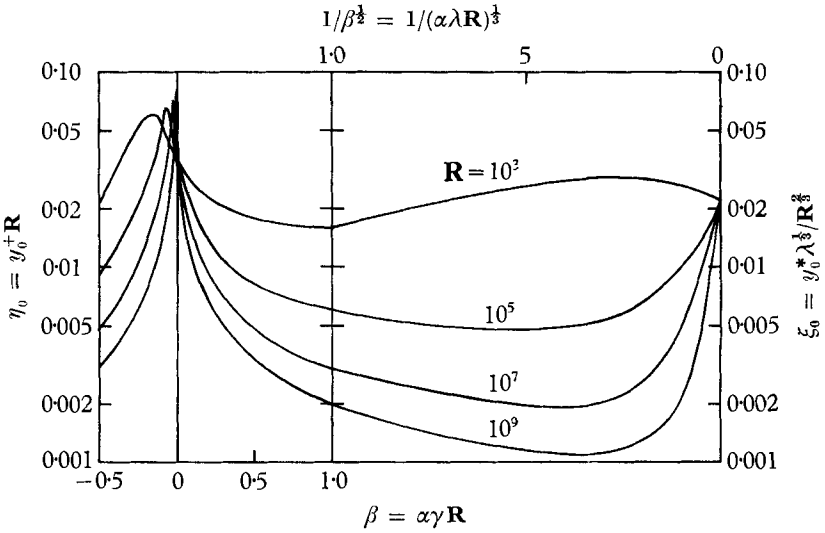


FIGURE 6. $\eta$ or $\xi$, which mark the outer edge of the velocity overlap layer. The outer edge is illustrated as point B in figure 7.

However, for small $\beta$ it has long been assumed in the literature that $\partial u/\partial y$ can be matched over a wide range, the importance of the logarithmic law of the wall residing in this assumption (or approximate experimental observation). This, of course, represents a sensible approach. We shall therefore replace the stipulation of a unique matching point with an outer limit where

$$|\tau_A - \tau_B|/\tau_B = 0{\cdot}05.$$

For $y$ smaller than this outer limit, agreement between $\tau_A$ and $\tau_B$ is, of course, much better. Values of $\eta$ (or $\xi$) corresponding to $|\tau_A - \tau_B|/\tau_B = 0{\cdot}05$ have been determined from the results of paper A and equation (11). These values are plotted in figure 6.

The stipulation of a 5% mismatch for $\tau$ and corresponding 2·5% mismatch for $\partial u/\partial y$ is therefore provided as a means of summing up our present discussion and as a guide to mark approximately the outer edge of the velocity overlap

† Except in the special cases $\beta = 0$ or $1/\beta = 0$. In the shear-stress plots of figures 6 and 7 in paper A the infinite slopes at $y = 0$ are not discernible. This is understandable since the slope changes rapidly and at $\eta_0 = y_0^+/\mathbf{R}$ has decreased to $\beta/\gamma$.

region. (This is strictly valid only for equilibrium layers. However, we suspect it might also serve as an approximate guide in the general case.) The inner edge, of course, coincides with the edge of the viscous sublayer.

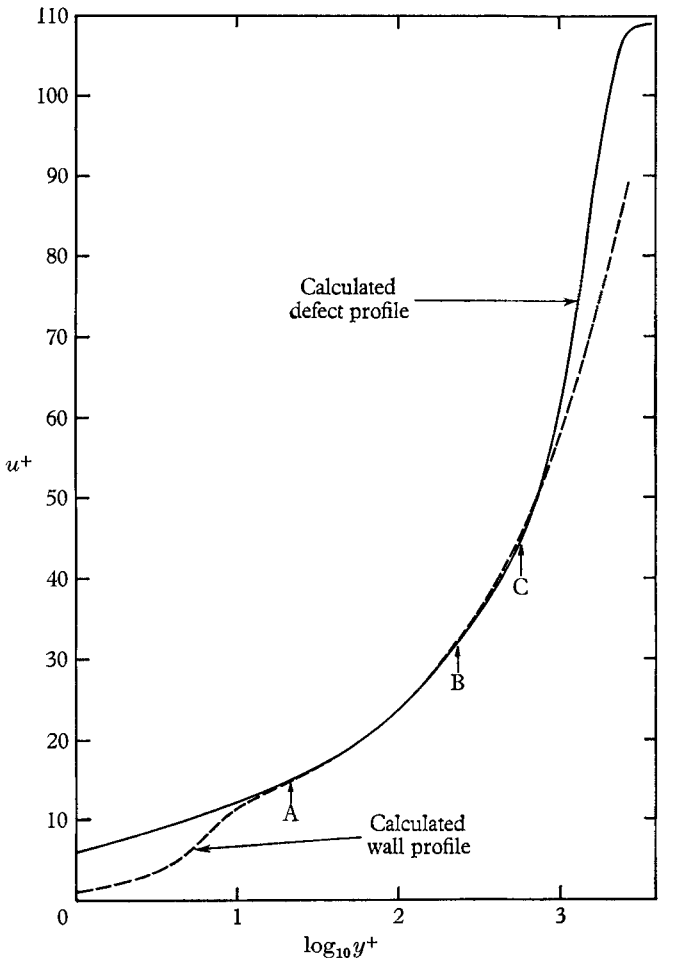


FIGURE 7. Illustration of the overlap of the wall and the defect layers for $\alpha = 0{\cdot}10$, $\mathbf{R} = 10^5$ and $\beta = 92{\cdot}5$. The points, A, B and C are described in the text.

In figure 7 we illustrate a specific example for $\alpha = 0{\cdot}10$ and $\mathbf{R} = 10^5$ (where $\beta = (\alpha\lambda\mathbf{R})^{\frac{3}{4}} = 92{\cdot}5$). On this plot we have marked the points A, B and C: A is the edge at the viscous sublayer; B marks the point where the linear-shear-stress approximation ceases to be valid according to the criterion above; C is the dividing point between the region where $\nu_e = \kappa^2 y^2 |\partial u/\partial y|$ and $\nu_e = KU\delta^*$ as in paper A. We have referred to the range A–C as the overlap layer or, what might be more explicit, as the effective viscosity overlap layer. A–B is then the velocity overlap layer; i.e. the overlap of defect velocity profiles of paper A and the wall profiles of the present paper.

## 7. Reconsideration of the skin-friction equation

It is finally possible to consider the skin-friction equation and to see if, or to what extent, equation (26) of paper A is valid. It was a result of paper A that to any specified accuracy there is a small enough value, $y = \epsilon$, where

$$U - u(\epsilon) = u_\tau A - \frac{u_\tau}{\kappa} \ln \frac{\epsilon}{\Delta}, \tag{20a}$$

and this result is correct even when $u_\tau = 0$. The results of paper A were calculated on the basis that, in the overlap layer, $\nu_e = \kappa^2 y^2 (\partial u/\partial y)$ so that $\kappa^2 y^2 (\partial u/\partial y)^2 = \tau/\rho$. We therefore obtain

$$u(y) - u(\epsilon) = \int_\epsilon \frac{(\tau/\rho)^{\frac{1}{2}}}{\kappa y}\, dy, \tag{20b}$$

valid within the overlap layer. Subtracting equation (20$b$) from (20$a$) and taking the limit, $\epsilon \to 0$, we obtain

$$U - u(y) = u_\tau A - \lim_{\epsilon \to 0} \left[ \frac{u_\tau}{\kappa} \ln \frac{\epsilon}{\Delta} + \int_\epsilon \frac{(\tau/\rho)^{\frac{1}{2}}}{\kappa y}\, dy \right]. \tag{20}$$

Equation (20) yields results in the overlap layer identical with those obtained in paper A.

If we now add equation (20) to equation (10), which is also applicable in the overlap layer, we obtain

$$U = u_\tau A + \frac{u_\tau}{\kappa} \ln \mathbf{R} + \lim_{\epsilon \to 0} \left[ \int_\epsilon \frac{\nu \psi(\chi)}{\kappa^2 y^2}\, dy - \frac{u_\tau}{\kappa} \ln \frac{\epsilon u_\tau}{\nu} \right]. \tag{21}$$

In the overlap layer, the last term may be identified (see equation (13$b$)) with $B^+$ so that the above equation may be written

$$\frac{1}{\gamma} = \left(\frac{2}{c_f}\right) = \frac{1}{\kappa} \ln \mathbf{R} + A + B^+, \tag{21a}$$

or

$$\frac{1}{\lambda} = \frac{1}{\kappa \beta^{\frac{1}{2}}} \ln \mathbf{R} + \frac{A}{\beta^{\frac{1}{2}}} + \frac{B^+}{\beta^{\frac{1}{2}}}, \tag{21b}$$

where $B^+/\beta^{\frac{1}{2}} = B^*/(\lambda \mathbf{R})^{\frac{1}{2}}$.

In paper A we have already determined $A(\beta)$. Combining this information with that of figure 4 enables us to plot both $A + B^+$ or $(A + B^+)/\beta^{\frac{1}{2}}$ as a function of $\beta$ and $\gamma$ or $\lambda$ as a function of $\beta$; these results are shown in figures 8 and 9, respectively.

*Uniqueness of $c_f$ for equilibrium flows*

Townsend (1961) has given analytical results pertaining to near-separating flows which indicate that, for essentially the same equilibrium flow and the same Reynolds number, two values of $\gamma = (c_f/2)^{\frac{1}{2}}$ (where one value might be zero) are possible. Presumably, the initial conditions would determine which of the two values are observed experimentally. Townsend further speculated that the flow corresponding to the larger value of $\gamma$ might be unstable in the sense that small initial-profile deviations would grow downstream. Alternatively, the flow corresponding to the smaller value of $\gamma$ would probably be stable.

All of this represents a rather interesting but complicated picture† and it is with some relief that we believe that we can disprove these contentions and replace them with the simple idea of a unique value of $\gamma$ for each equilibrium flow.

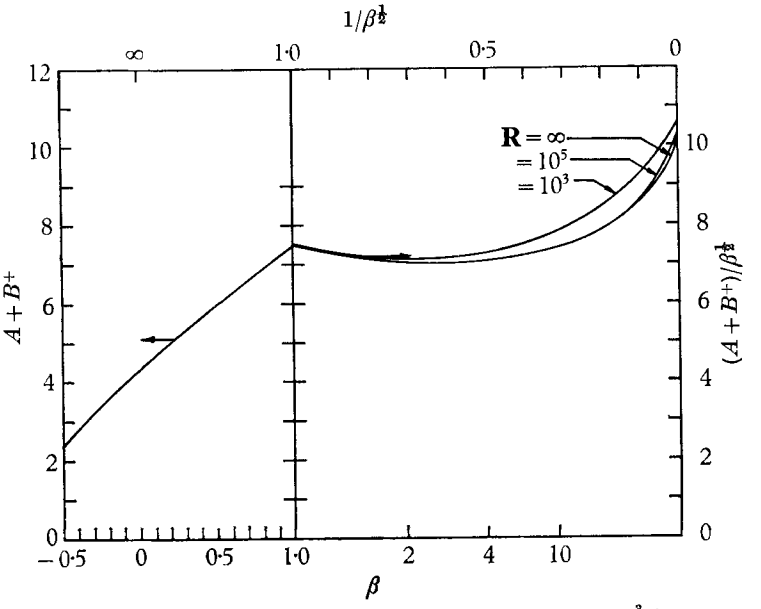


FIGURE 8. The combination $A+B^+$. Since $B^+ = B^+(\alpha)$ and $\alpha = (\beta^{\frac{3}{2}}/\lambda\mathbf{R})$, the curve for $\mathbf{R} = \infty$ corresponds to $B^+ = B^+(0) = 4{\cdot}9$ and is simply related to figure 8 of paper A.

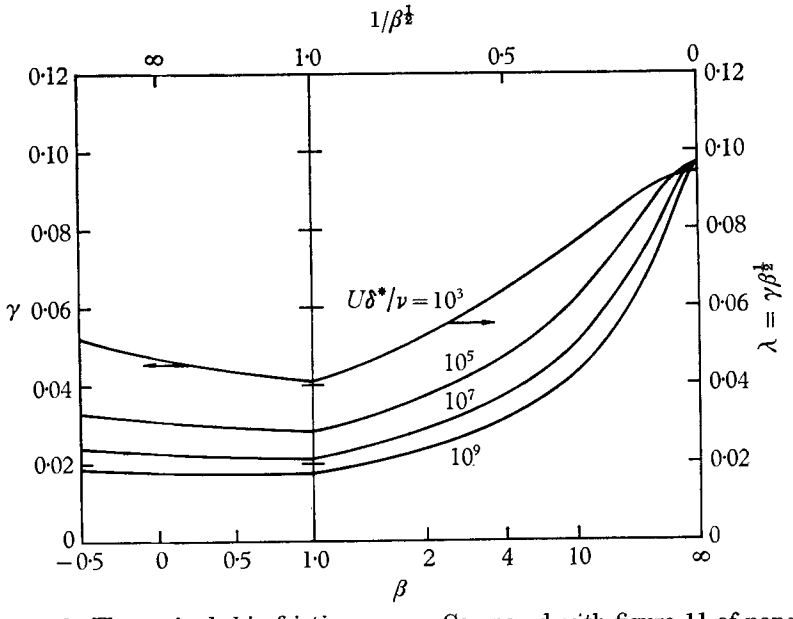


FIGURE 9. The revised skin-friction curve. Compared with figure 11 of paper A a unique value of $\gamma$ is obtained for each equilibrium flow.

† We have already looked into the possibility of a general non-equilibrium theory based on the present work. Indications are that non-uniqueness for $\lambda(\beta, \mathbf{R})$ would represent a rather serious impediment to the determination of separation in the general case.

The difficulty can be recognized in paper A for there we found that for large $\beta$ the main-stream velocity distribution for an equilibrium flow could be written as

$$\frac{U}{U_0} = \left[1 - \frac{\lambda^2}{m}\frac{x}{\delta_0^*}\right]^m,$$

where $U_0$ and $\delta_0^*$ are the initial values of $U$ and $\delta^*$. Since $m$ varies only slightly about the value $-0{\cdot}230$ the flow is almost completely determined by $\lambda^2 = (\delta^* dp/dx)/\rho U^2$ as one might expect when $\tau_0$ is very small. If one now refers to figure 11 of paper A one will see (when $1/\beta^{\frac{1}{2}}$ is small) that, for the same values of $\mathbf{R}$ and $\lambda$, two values of $1/\beta^{\frac{1}{2}} = \gamma/\lambda$ and therefore $\gamma$ are possible. This would support Townsend's findings. But it is just this point that has been amended in the present paper as will be seen in the revised plot of the present paper, figure 9; here there exists a unique value of $1/\beta^{\frac{1}{2}} = \gamma/\lambda$ and therefore $\gamma$ for each value of $\lambda$ and $\mathbf{R}$.

The previous false result was obtained by maintaining $B^+ = 4{\cdot}9$ so that, using equation (52) of paper A, we found that for large $\beta$

$$\frac{1}{\lambda} = \frac{1}{\kappa\beta^{\frac{1}{2}}}\ln \mathbf{R} + 10{\cdot}27 + \frac{1}{\kappa\beta^{\frac{1}{2}}}\ln\left(\frac{0{\cdot}101}{\beta^{\frac{3}{2}}}\right) + \frac{4{\cdot}9}{\beta^{\frac{1}{2}}}. \tag{22}$$

The third term in equation (22) is responsible for the appearance of a maximum in the curve $\lambda(\beta^{-\frac{1}{2}})$ for each $\mathbf{R}$ as shown in figure 11 of paper A. But, if we now incorporate a variable $B^+$ or $B^*$ as determined by equation (32) of appendix A in the present paper, we find, after some rearranging, that

$$\frac{1}{\lambda} = 10{\cdot}27 + \frac{1}{\kappa\beta^{\frac{1}{2}}}\ln\left(\frac{0{\cdot}101}{4\lambda}\right) + \frac{1{\cdot}33}{(\lambda R)^{\frac{1}{3}}}. \tag{23}$$

(We have here only incorporated the largest terms in equation (32).) Equation (23) like figure 9 of the present paper displays no maximum and a single value of $\lambda$ corresponds to a single value of $\beta$ for a given Reynolds number.

## 8. Reconsideration of Stratfold's data

We have re-examined Stratford's (1959) data in the light of the present work. In paper A we encountered a need to assume a 'zero slip' condition. This need is now eliminated. This time we have accurately (within 5 %) determined the *local* experimental values of $\lambda^2 = (\delta^*/\rho)(dp/dx)$. With $\lambda$ and $\mathbf{R}$ known at every $x$ it is possible to recast the data in the form $u^*(y^*)$ (where $u^* = (\mathbf{R}/\lambda^2)^{\frac{1}{2}}(u/U)$ and $y^* = (\mathbf{R}\lambda)^{\frac{1}{2}}(y/\delta^*)$), and this is how the data are presented in figure 10.

Next the calculated wall profiles are drawn. The shear stress and therefore $1/\alpha$ are not known *a priori*. However, if one relies on the theory, $1/\alpha$ can be determined by comparison of theory and data. In figure 10(*a*) we have chosen $1/\alpha = 0{\cdot}5$; in figure 10(*b*) one might be tempted to draw in a curve corresponding to a slightly *negative* $\tau_0$ or $\alpha^{-\frac{2}{3}}$. However, in the present paper we have not yet generalized the theory to include separated flows. It is nevertheless apparent that both flows correspond to $1/\alpha \simeq 0$. It should be noted that the data points at $y^{*\frac{1}{2}} \simeq 2$ required that the probe rest on the wall so that the outside probe

dimension (the probe was flattened) is $y_p^* \simeq 8$. It is not only possible, but highly probable, that the measurements were subject to streamline probe shifts† as is apparent in figure 10. The calculated defect profiles may also be plotted in figure 10 ($u^* = \mathbf{R}^{\frac{1}{3}}\lambda^{\frac{1}{3}}\{1/\lambda - F'(\xi)\}$ and $y^* = \xi\mathbf{R}^{\frac{2}{3}}/\lambda^{\frac{1}{3}}$. Note that, for large enough

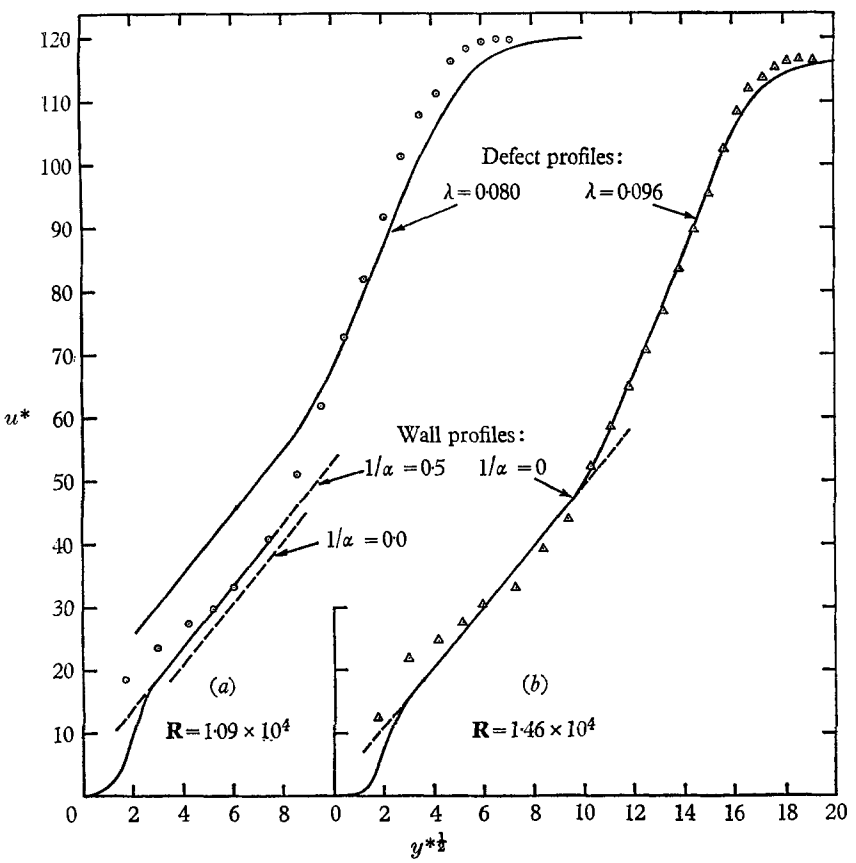


FIGURE 10. A detailed comparison of Stratford's data with theory. The symbols used are the same as in figure 5 of paper A. The profile of figure 10(*a*) is approaching equilibrium while the profile of figure 10(*b*) is almost precisely in equilibrium.

$\beta$, $F'(\xi)$ is sensibly invariant with $\beta$.) We now observe that the wall profile and the defect profile do not match in figure 10(*a*) whereas they do in figure 10(*b*). Also, from the equilibrium value, $1/\beta = 0{\cdot}04$, determined from figure 9 we obtain $1/\alpha = \lambda\mathbf{R}/\beta^{\frac{3}{2}} \simeq 7$ in disagreement with the value $1/\alpha \simeq 0{\cdot}5$ required by the wall layer in figure 10(*a*).

† We had originally included in our analysis a correction to the effective viscosity proposed by Townsend (1961). The correction involved $\partial\tau/\partial y$ or $\partial^2 u/\partial y^2$. One effect of the correction is to alter the effective $\kappa$ in the expression $u^* = \text{const.} + (2/\kappa)y^{*\frac{1}{2}}$ for small $1/\beta$. From Stratford's data, Townsend determined that $\kappa \simeq 0{\cdot}5$ instead of 0·41. But in his determination Townsend included the points near the wall which we believe are subject to probe shift. From the present comparison we might conclude that, at most, $\kappa = 0{\cdot}44$. In any event, the correction would only slightly modify our results quantitatively and not at all qualitatively.

All of this is extremely interesting since we believe that in figures 10(*a*) and 10(*b*) we are observing the flow in its *adjustment* to equilibrium. To exploit this further we have prepared figure 11. In figure 11(*a*) values of $\lambda$ are determined with fairly good accuracy from the data. In figure 11(*b*) we have plotted curves of $\alpha^{-\frac{2}{3}}$. The curve labelled 'Actual value' is obtained by comparison of the

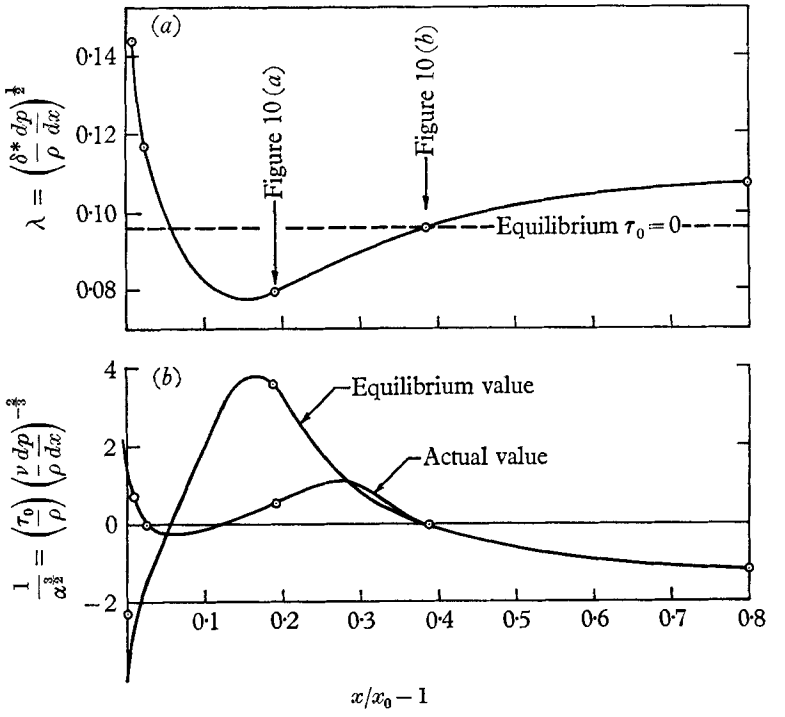


FIGURE 11. A sketch illustrating the approach to equilibrium. The actual value of $\alpha^{-\frac{2}{3}}$ lags the value according to the equilibrium theory.

theoretical wall profiles with the data near the wall. The curve labelled 'Equilibrium value' is obtained from the experimental values of $\lambda$, figure 9, and the expression $\alpha^{\frac{2}{3}} = (\lambda \mathbf{R})^{\frac{2}{3}}/\beta$. It will be appreciated that the curves drawn in figure 11(*b*) are highly imaginative† but the picture that emerges is that the actual value of the shear stress or $\alpha^{-\frac{2}{3}}$ lags the value which would have been obtained if the flow were in equilibrium (approximately specified by $\lambda(x) = \text{const.}$) with the same value of $\lambda$. We believe that these comments might be a precursor to a general theory which accounts for the observed lag effect.

## 9. Conclusions

An effective viscosity hypothesis is presented which, it would appear, is universally applicable to all turbulent flows near a smooth wall. Evidence is presented which indicates that other hypotheses that have appeared in the literature are either restricted to small pressure gradients, or to smaller portions of the layer.

† The negative values of $\alpha^{-\frac{2}{3}}$ are obtained by a rather gross extrapolation of our present theory, although it is possible to say that they are indeed negative.

The effective viscosity hypothesis when combined with the findings of paper A is summarized in figure 3. By stipulating $\mathbf{R} = U\delta^*/\nu$ a single, continuous function, $\phi(\zeta)$ or $\Phi(Z)$ is obtained.

It would have then been possible to determine a single solution for the complete velocity profile for each $\mathbf{R}$ and $\beta = \delta^*(dp/dx)/\tau_0$. However, we found that it was also possible to split the solution so that,

$$\left.\begin{aligned} &\text{for the defect layer,} \quad (U-u)/u_\tau = f'(y/\Delta, \beta); \\ &\text{and, for the wall layer,} \quad u/u_\tau = u^+(u_\tau y/\nu, \alpha), \end{aligned}\right\} \tag{24}$$

where $\alpha = \nu(dp/dx)/\rho u_\tau^3$. The separate velocity profiles may also be presented in alternative forms which remain finite as $u_\tau \to 0$.

For given values of $\beta$ and $\mathbf{R}$ the defect profile automatically overlaps a portion of the wall profile. As illustrated in figure 7 the velocity overlap portion need not be logarithmic. Nevertheless, $U/u_\tau \equiv (2/c_f)^{\frac{1}{2}} = f' + u^+ = fcn(\beta, \mathbf{R})$ so that a comparatively simple skin-friction equation is obtained directly.

Research was carried out with BuShips Hydromechanics Research Program S-R009 01 01 administered by the David Taylor Model Basin Contract Number Nonr-(1858) 38. This work made use of Computer Facilities supported in part by National Science Foundation Grant NSF-GS 579.

## Appendix A: Evaluation of $B^*$ in the neighbourhood of $1/\alpha = 0$.

We wish to evaluate

$$B^* = \frac{B^+}{\alpha^{\frac{1}{3}}} = \lim_{\epsilon \to 0} \left[ \int_\epsilon^a \frac{\psi(\chi)}{\kappa^2 y^{*2}}\, dy^* - \frac{1}{\kappa \alpha^{\frac{1}{3}}} \ln \frac{\epsilon}{\alpha^{\frac{1}{3}}} \right], \tag{25}$$

where $a$ is a value of $y^*$ outside the viscous sublayer (where $\psi = 0$). We now define a quantity, $b$, such that

$$b \gg 1/\alpha^{\frac{2}{3}}, \tag{26}$$

and split up equation (25) so that

$$B^* = \lim_{\epsilon \to 0} \left[ \int_\epsilon^b \frac{\psi(\chi)}{\kappa^2 y^{*2}}\, dy^* - \frac{1}{\kappa \alpha^{\frac{1}{3}}} \ln \frac{\epsilon}{\alpha^{\frac{1}{3}}} \right] + F(b), \tag{27}$$

where

$$F(b) = \int_b^a \frac{\psi(\chi)}{\kappa^2 y^{*2}}\, dy^*$$

is approximately a function of $b$ and not of $\alpha$ since $\chi = \kappa(\alpha^{-\frac{2}{3}} + y^*)^{\frac{1}{2}} y^* \simeq \kappa y^{*\frac{3}{2}}$. Now, if we further restrict $b$ so that approximately

$$3 > b, \tag{28}$$

then in the range $0 \leqslant y^* < b$ it may be ascertained from figure 2 that

$$\psi(\chi) \simeq -\chi + \chi^2.$$

(This behaviour for small $\chi$ can be obtained from the discussion of § 6) and the integral in equation (27) may be evaluated analytically as

$$B^* = -\frac{2}{\kappa}[(\alpha^{-\frac{2}{3}} + b)^{\frac{1}{2}} - \alpha^{-\frac{1}{3}}] - \frac{1}{\kappa \alpha^{\frac{1}{3}}} \ln \left[ \frac{4\,(\alpha^{-\frac{2}{3}} + b)^{\frac{1}{2}} - \alpha^{-\frac{1}{3}}}{\alpha\,(\alpha^{-\frac{2}{3}} + b)^{\frac{1}{2}} + \alpha^{-\frac{1}{3}}} \right] + \frac{b}{\alpha^{\frac{2}{3}}} + \tfrac{1}{2} b^2 + F(b). \tag{29}$$

Now at $\alpha = \infty$ we have

$$B^*(\infty) = -2b^{\frac{1}{2}}/\kappa + \tfrac{1}{2}b^2 + F(b), \tag{30}$$

so that, subtracting equation (30) from (29), we obtain

$$B^* = B^*(\infty) - \frac{2}{\kappa}\left[(\alpha^{\frac{2}{3}}+b)^{\frac{1}{2}} - \alpha^{\frac{1}{3}} - b^{\frac{1}{2}}\right] + \frac{b}{\alpha^{\frac{2}{3}}} - \frac{1}{\kappa\alpha^{\frac{1}{3}}}\ln\left[\frac{4}{\alpha}\frac{(\alpha^{-\frac{2}{3}}+b)^{\frac{1}{2}} - \alpha^{-\frac{1}{3}}}{(\alpha^{-\frac{2}{3}}+b)^{\frac{1}{2}} + \alpha^{-\frac{1}{3}}}\right], \tag{31}$$

where $B^*(\infty) = 1{\cdot}33$ has been evaluated numerically.

If we now expand equation (31) for small $1/\alpha^{\frac{1}{3}}$ we obtain

$$B^* = B^*(\infty) - \frac{1}{\kappa\alpha^{\frac{1}{3}}}\ln\frac{4}{\alpha} + \frac{2}{\kappa}\frac{1}{\alpha^{\frac{1}{3}}} + \left(b + \frac{1}{\kappa b^{\frac{1}{2}}}\right)\frac{1}{\alpha^{\frac{2}{3}}}, \tag{32}$$

which indicates that the final result is fairly insensitive to $b$ as $1/\alpha^{\frac{1}{3}} \to 0$ and it is only the first two terms in equation (32) that are important. Nevertheless, if we set $b = 3$ we find that equation (32) is accurate to the second significant figure in the range $0 \leqslant 1/\alpha^{\frac{1}{3}} \leqslant 0{\cdot}5$.

## REFERENCES


Deissler, R. G. 1959 Convective heat transfer and friction in flow of liquids. *High Speed Aerodynamics and Jet Propulsion*, vol. 5, pp. 288–338. Princeton University Press.

Ferrari, C. 1956 Wall turbulence. *NASA RE* 2-8-59 W.

Laufer, J. 1954 The structure of turbulence in fully developed pipe flow. *NACA Rep.* no. 1174.

Millikan, C. B. A. 1938 A critical discussion of turbulent flows in channels and circular tubes. *Proc. Fifth Inter. Congr. Appl. Mech.*, pp. 386–392.

Mellor, G. L. & Gibson, D. M. 1966 Equilibrium turbulent boundary layers. *J. Fluid Mech.* **24**, 225.

Stratford, B. S. 1959 An experimental flow with zero skin friction throughout its region of pressure rise. *J. Fluid Mech.* **5**, 17–35.

Townsend, A. A. 1956 *The Structure of Turbulent Shear Flow.* Cambridge University Press.

Townsend, A. A. 1961 Equilibrium layers and wall turbulence. *J. Fluid Mech.* **11**, 97–120.

Van Driest, E. R. 1956 On turbulent flow near a wall. *J. Aero Sci.* **23**, 1007.

Van Driest, E. R. & Blumer, C. B. 1963 Boundary layer transition: freestream and pressure gradient effects. *AIAA J.* **1**, 1303–1306.